China Geology 7 (2024) 672−685

China Geology

Journal homepage: http://chinageology.cgs.cn
https://www.sciencedirect.com/journal/china-geology

Estimation and mapping of water erosion and soil loss: Application of Gavrilovic erosion potential model (EPM) using GIS and remote sensing in the Assif el mal Watershed, Western high Atlas

Kabili Salma[a,*], Algouti Ahmed[a], Algouti Abdellah[a], Ezzahzi Salma[a]

[a] *The University of Cadi Ayyad, Faculty of Sciences Semlalia, Department of Geology, Geoscience Geotourism Natural Hazards and Remote Sensing Laboratory (2GRNT), Marrakech 40000, Morocco*

A R T I C L E   I N F O

Article history:
Received 5 June 2023
Received in revised form 28 August 2023
Accepted 5 September 2023
Available online 5 January 2024

Keywords:
Water erosion
Soil degradation
Risk
Assif el mal watershed
EPM
GIS and remote sensing
Map
Morocco
Digital elevations models

A B S T R A C T

Water erosion is a serious problem that leads to soil degradation, loss, and the destruction of structures. Assessing the risk of erosion and determining the affected areas has become crucial in order to understand the main factors influencing its evolution and to minimize its impacts. This study focuses on evaluating the risk of erosion in the Assif el mal watershed, which is located in the High Atlas Mountains. The Erosion Potential Model (EPM) is used to estimate soil losses depending on various parameters such as lithology, hydrology, topography, and morphometry. Geographic information systems and remote sensing techniques are employed to map areas with high erosive potential and their relationship with the distribution of factors involved.Different digital elevation models are also used in this study to highlight the impact of data quality on the accuracy of the results. The findings reveal that approximately 59% of the total area in the Assif el mal basin has low to very low potential for soil losses, while 22% is moderately affected and 19.9% is at high to very high risk. It is therefore crucial to implement soil conservation measures to mitigate and prevent erosion risks.

1. Introduction

Soil erosion is a natural phenomenon affecting harmfully soil, it is one of the most important causes of land degradation and one of the important keys to global environmental hazards (El Mouatassime S et al., 2019). Erosion is generally defined as the process of soil separation and loss caused by the dynamic effects of several agents like wind and water, which is the origin of sediments production available subsequently for transport. Soil degradation by erosion poses serious economic, social and environmental problems in several regions of the world and more particularly in the Mediterranean regions (Zahnoun A and Al Karkouri, 2020; Liu GD et al., 2023).

The dominant geomorphological process in most of the globe is due in particular to water erosion (Toy TJ et al. 2002) caused by rainfall, melted snow, or runoff, water erosion remains an important risk which effects, can affect dynamically balanced watershed systems indirectly by increasing water runoff and degrade water quality and cause maldistribution of water in the watershed (Black PE, 1984; Amini S, 2010).

The high atlas of Morocco is globally a representative example of an unprotected area that suffers from the harmful impact of erosion on its environment (Fig. 1). Known by its high reliefs, its diversified geology and lithology as well as its hierarchical hydrographic network, it exposes all the forms of water erosion which impacts differs. Human development and the inappropriate land utilization have accelerated the soil erosion at many locations on the earth's surface (El badaoui K et al., 2021). As a result, every year millions of tons of sediment are produced around the world, and the water erosion is responsible for more than 56% of this sediment volume (Elirehema Y, 2001).

The objectives of this study are the determination of soil losses and the detection of areas with high susceptibility to erosion using the EPM model which is defined by the mapping of important factors controlling it. The study of this phenomenon and its consequences depending on the area have

* Corresponding author: *E-mail address*: salma.kabili@edu.uca.ma (Kabili Salma).

Literary editor: Xi-jie Chen
doi:10.31035/cg2023058
2096-5192/© 2024 China Geology Editorial Office.

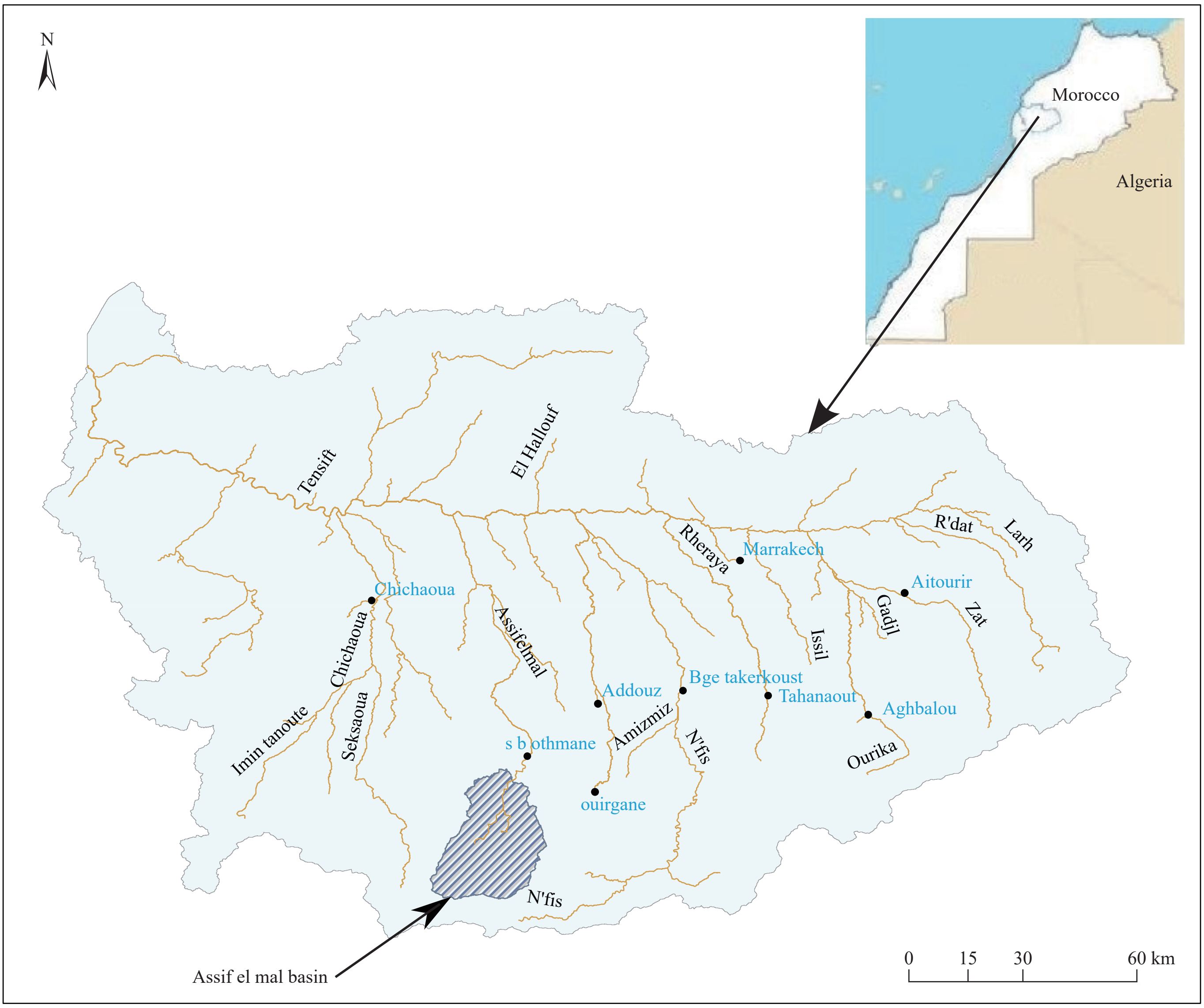

Fig. 1. Geographical location of the Assif el mal watershed.

proven to be essential in purpose of limiting its affects and preventing solutions to decrease its evolution.

The applications of Geographic Information Systems (GIS) and remote sensing techniques in erosion have been developed recently, by using several physical or empirical models that consider soil erosion in watersheds, it became possible to locate erodible area and assess erosion susceptibility by determining all the parameters involved as soil characteristics and external factors controlling it. One of these models is Erosion Potential Method (EPM) (Gavrilovic S, 1957, 1966, 2008, 1972), this empirical model also known as the Gavrilovic method, is widely used to estimate sediment yield and soil erosion severity on catchment scale. The model is commonly used due to its simplicity and ease of use, it helps predict the erosion potential in different temporal and spatial scales, by providing quick results with availability of data, it gives a rapid assessment of the erosion potential, allowing for timely decision-making and mitigation measures. Otherwise, the use of this model, such as other empirical models, can be interfered by various hindrance. Accordingly, the model assumes a simplified representation of the complex processes involved in erosion, which can result in some inaccuracies and limitations. It also requires accurate data on various factors such as topography, soil properties, and vegetation cover, which may not always be readily available, especially in remote or underdeveloped regions. And although the data are available, their source may be unclear and less detailed. The assessment of erosion in larges scales can consequently cause lack of consideration of local factors specific characterizes of the concerned area which make it less suitable.

The EPM considers six individual factors, depending on the aggressiveness of precipitation, the slope and the length of the slope, the erodibility of the soil, the vegetation cover and the cultural practices, which are the main factors that control water erosion. Each factor exhibits different behavior from one area of the watershed to another. The spatial analysis of this behavior thus leads to a multitude of data that must be mapped, stored, structured and processed rationally (Sadiki A et al., 2009).

Each parameter was discussed individually in relation to its effect upon the method results, and ranked into categories depending on their influence (El badaoui K et al., 2021), then superimpose them in GIS to establish a quantitative map exposing water erosion and its affects for each zone.

The implementation of this methodology has been widespread in several countries (Serbia, Croitia, Slovania, Italy, Greece et al.) (Efthimiou N and Lyoukdi E, 2016) and nowadays all over the countries. In Morocco, this methodology was adopted in various regions (Toudgha river southeast of Morocco (El badaoui K et al., 2021), Boumlal wadi-central rif of Morocco (El bouali A et al, 2017), Rheraya watershed-High Atlas of Morocco (Kabili S et al, 2023), Oued Tleta-Western Rif, Morocco (Zahnoun A and Al Karkouri, 2020) giving reliable results. So considering the above, this study aimed to evaluate the performance of EPM and the input data at the level of the Assif el mal basin.

2. Study area

The Assif el mal watershed is situated in the middle of the High Atlas and is part of the large Tensift basin. It is located at a hundred kilometers south-west of the city of Marrakech, precisely between the cities of Imi-n-tanout and Amezmiz. The basin is characterized by its oval shape with an area of 224 km² and endowed with slightly dense hydrographic Network imbued with a weak and irregular flow coming from the confluence of two main affluents, which are Assif el mal and Assif Tiguenarine.

The Assif El Mal watershed features elevations spanning from 953 m to 3500 m, characterized by predominantly steep slopes and rugged geology. This is attributed to its position within the Hercynian segment of the High Atlas chain. The climate of the area is mainly continental of semi-arid arid type influenced by the presence of the High Atlas relief giving sometimes an annual average rainfall of more than 700 mm upstream (Fig. 2). Moreover, the vegetation in the basin is not very dense and most of the surface of the area appears as bare soil with little grass. The hydrographic network of the basin practically dense with a weak flow presenting irregularity (Kabili S et al., 2023).

3. Materials and methods

In order to study the dynamics of erosion and quantify soil losses in the Assif el mal watershed we will use the erosion potential method - EPM (Gavrilovic S, 1972), which was developed in the 1950s by Gavrilovic. It is based on the combination of factors affecting water erosion in a watershed including rainfall, temperature, soil sensitivity, soil protection, types of erosion and slopes. Soil losses are quantified by the equations developed by Gavrilovic (Zahnoun A and Al Karkouri, 2020). The quantification of erosion in the basin of Assif el mal following this methodology has highlighted the annual sediment yield and transport, the forms and intensity of erosion from the geographic, physical, meteorological and hydrological characteristics of the river basin (Kabili S et al., 2023).

The modeling of these factors will be done using Arcgis software, by establishing a map showing the distribution and influence of each factor in the basin of Assif el mal. By combining this data, we will obtain an estimation of the erosion potential in the area, which is linked to the impacts of various parameters contributing to this phenomenon, related to the effects of the different parameters responsible of this fact. The mapping of erosion in the basin of Assif el Mal has highlighted the most exposed sectors to erosion, as well as the various risks associated with this phenomenon (Kabili S et al., 2023).

In the present study three types of open source DEMs with different resolution, precision and coverage were acquired and tested to assess the impact of their accuracy when estimating erosion using erosion potential model. DEMs are needed to estimate topographic characteristics of watersheds such as: slope length, hypsometry, channel network, Topographic Wetness Index, relative relief, drainage density (Da ros D and Borga M, 1997).

Applying the EPM method will not only illuminate erosion within the basin but also assess its impact when these sources are taken into account and thus evaluate the influence of their qualities on the relevance of the results. The quality of a DEM is affected by different types of errors and changes with terrain conditions (Kishan SR et al., 2012).

This approach aid to evaluate and thus to propose the best source to use with remote sensing methods, related to the characterization of natural hazards. The quality is assessed by taking into account DEM usability and by its representational, qualitative, and intrinsic features (Khal M et al., 2020).

Digital Elevation Models (DEMs) play a significant role in influencing various essential parameters for terrain analysis, land management, and erosion assessment within a region. These parameters encompass aspects such as slope, curvature, hydrological analysis, flow accumulation, landform identification, sediment transport modeling, land use planning, and erosion potential.

The spatial distribution of parameters of the Assif el mal basin derived from diverse sources of DEM data is characterized by distinct features and variations. The resolution of DEMs plays a pivotal role: higher-resolution DEMs capture finer details, resulting in more precise parameter calculations. For instance, parameters like slope, aspect, and curvature exhibit increased variability and detail within their spatial distribution when derived from higher-resolution DEMs. In contrast, coarser-resolution DEMs tend to smooth out features, yielding less intricate spatial patterns.

Moreover, the accuracy of DEMs directly influences the reliability of derived parameter values. Accurate DEMs reflect spatial patterns that align better with the actual terrain characteristics. Inaccuracies in DEM data can lead to skewed spatial distributions, potentially misrepresenting the landscape features. The method of acquiring data from each source also contributes significantly, with various methods like Lidar, satellite imagery, and aerial photography introducing

Fig. 2. (a)–Different formations of the Assif el mal basin. C.T–Cenomanian-Turonian dolomitic limestone; IC–Infra-Cenomanian with detrital red formation; AA–Apto Albian: Marl-limestone; Dogger–detrital red formation; Lias–Carbonato-evaporitic; Cambrian–schists and sandstones. (b)– Example of aspects of erosion in the Assif el mal basin: Landslide leading to blockage of the road; (c)–Rockfalls reaching the top of a village; (d)–Erosion of the banks and transport of sediments by wadi.

variations in DEM quality. Lidar-generated DEMs provide highly accurate elevation data, resulting in more realistic spatial patterns for parameters. In contrast, DEMs derived from optical imagery can be influenced by shadows, vegetation, and atmospheric conditions, leading to spatial distributions influenced by these factors.

The specific attributes of terrain, such as steepness, roughness, and complexity, interact with DEM resolution and accuracy to shape the spatial distribution of parameters. Higher-resolution DEMs excel in capturing intricate terrain features, unveiling subtle spatial patterns in parameter distributions.

As a result, the spatial distribution of parameters from different DEM data sources exhibits varying levels of detail, accuracy, and realism. Higher-resolution and more accurate DEMs tend to generate spatial distributions that closely mirror the actual terrain, whereas coarser or less accurate DEMs might simplify features and introduce distortions. Recognizing these characteristics aids in interpreting parameter distributions and making informed decisions based on the strengths and limitations of the data source.

The workflow is illustrated in the following figure (Fig. 3), showing the succession of the different steps of the methodological approach of the EPM model of Gavrilovic applied for the elaboration of the soil loss map, which gives an estimate of erosion in (m^3/km^2/year). It is based on multisource data such as the geological map, satellite images, three DEMs (Aster 30 m, Srtm 30 m, and Alos Palsar 12.5 m) added to the field work. The integration of these parameters in the GIS allowed to easily quantify the extent of erosion and its spatialization in the Assif el mal basin and showed at the same time the influence of the quality of the data and sources used on the accuracy of the results.

The elaboration of the soil loss map was done directly on ArcGIS by calculating first the erosion coefficient Z based on the following equation:

$$Z = Y \times X_a \times (\Phi + J_a^{1/2}) \quad (1)$$

Using the data of:

- Soil sensitivity (Y) depending on the structure and constitution of the soil being a major and fundamental element in its resistance, this factor is calculated from the following equation:

$$Y = 2.1 \times M^{1.14} \times 10^{-4} \times (12 - A) + 3.25(B - 2) + 2.5(C - 3)/100 \quad (2)$$

Where: M=(% Fine sand+silt)×(100−% Clay); A: percentage of organic matter; B: the code the soil structure (1 to 6); C: permeability classes;

- Slope (J_a) calculated from three different digital terrain models

- Soil protection (X_a) determined from land use and strongly influenced by the presence of the vegetation

- Erosion types and extent (Φ) are determined by the degree of erosion and the process that caused it.

Then, in the similar way, we were able to elaborate the soil loss map (W) in the Assif el mal basin.

$$W = (Z^{3/2}) \times T \times H \times \pi \quad (3)$$

By adding the average annual rainfall data (H) temperature data (T) calculated using the following equation,

$$T = ((0.1 \times (t_o) + 0.1) \quad (4)$$

Where T is the Coefficient of temperature and to represents the average annual temperature.

4. Results and discussions

4.1. Results

4.1.1. Soil sensitivity

Soil sensitivity to erosion refers to the vulnerability to erosion due to lithological and climatic conditions. The map depicting soil sensitivity to erosion was generated by applying equation (2) and incorporating key criteria that characterize the soil composition of each formation. These criteria encompass texture, structure, permeability, and organic matter content, in conjunction with lithological data.

To establish these inherent properties, the laser particle size analysis was initially conducted to ascertain the proportions of various particle size fractions (sand, silt, clay) within samples. This facilitated the determination of structure and permeability codes by plotting these parameters on texture diagrams (Fig. 4). Subsequently, the organic matter content was determined using the fire loss method (Table 1). The culmination of these analyses provided us with a comprehensive understanding of the susceptibility of each formation to erosive agents, derived from the mentioned assessments (Fig. 5).

The map illustrates the composition of the Assif el Mal

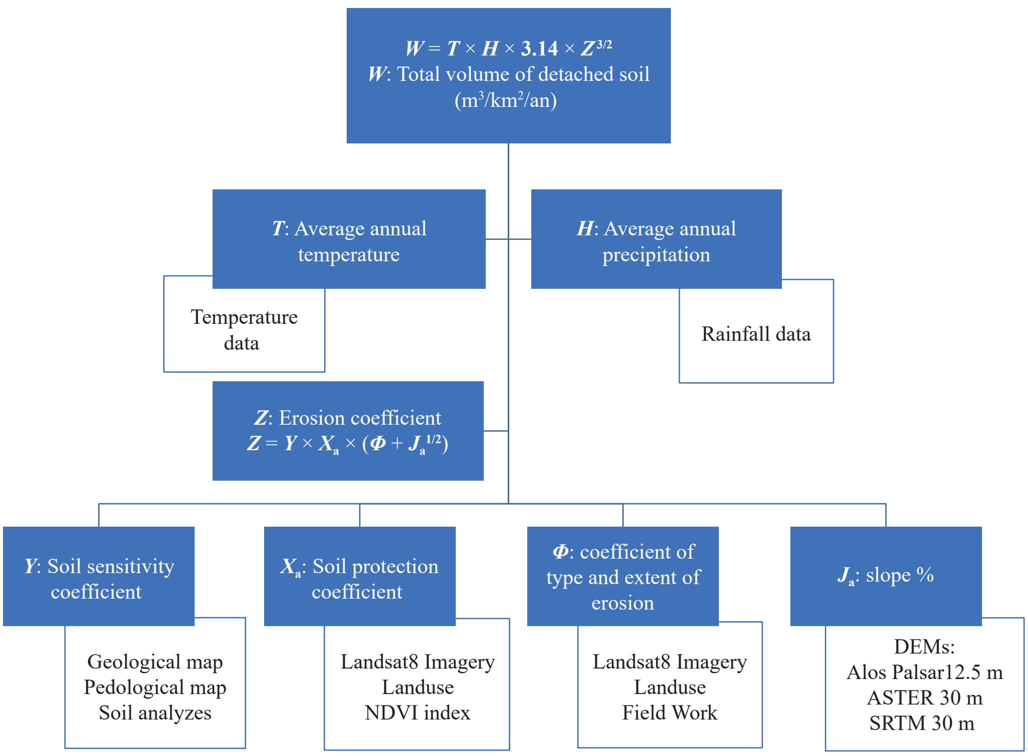

Fig. 3. Methodological approach of the EPM model.

basin which is mostly predominated by soils susceptible to erosion. This fits perfectly with the lithological data in which it has already been shown that the basin consists in large part of fragile metamorphic schistose formations.

4.1.2. Temperature Coefficient (T)

The temperature is an essential factor of erosion in the EPM model, its importance is marked by its effect on water in the soil by controlling evaporation and transpiration.

The temperature data has been acquired directly from the NASA website, power.larc.nasa.gov, which provides precipitation, humidity, and air temperature data gathered through meteorological satellites. The annual average temperature data of five different stations was then applied in the equation (4), and shows that the temperature coefficient at the level of the Assif el mal basin varies between 1.635°C and 1.995°C (Table 2). These coefficients are employed to create a temperature map using the ArcGIS software, utilizing the Spline interpolation method (Fig. 6). The results presented in the map showcase the differentiation in air temperature degrees based on spatial scales. However, the precision of the map derived from this application remains low, which partially influences the accuracy of the results during the compilation of all data.

4.1.3. Precipitations (H)

Precipitation plays a very important role in erosive dynamics. They directly contribute to the triggering of runoff and transportation of materials. The duration and intensity of precipitation are decisive in determining or assessing the quantities of eroded materials (El bouhali A, et al., 2017).

The Assif el mal basin has a semi-arid climate and a seasonally variable rainfall system. To estimate the annual precipitation H, we used data collected from different meteorological and rainfall stations (Table 3) spread across the basin provided by the agency of hydraulic basin of Tensift (ABHT). The interpolation of these values following the Spline methodology allowed the establishment of the map (Fig. 7) which shows that the basin experiences a variation in the intensity of precipitation whose gradient decreases from upstream to the outlet, which allows us to conclude the presence of a significant erosive potential upstream. However, the map's accuracy appears to be low, which will certainly affect results.

4.1.4. Soil protection coefficient (X_a)

This factor is generally related to the occupation of the soil and especially to the presence of vegetation, which protects the soil from erosion in several ways especially by stabilizing and protection it during rainfall and runoff and also by increasing the permeability of the soil.

In the framework of Gavrilović's EPM model, the coefficient of soil protection derives its significance from both land use patterns and the presence of vegetation. Gavrilović's

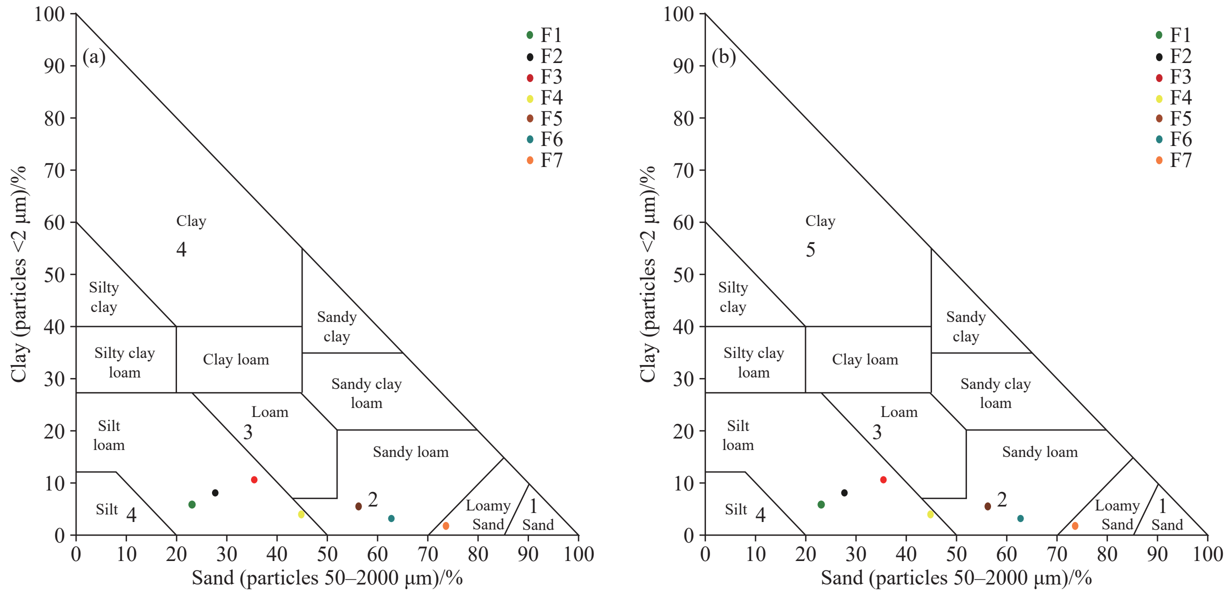

Fig. 4. Triangular diagram based on texture classification indicating: (a) the code of permeability and (b) the code of structure.

Table 1. ***Y*** **coefficient generated from the results of the sedimentological analyses.**

Samples	Clay/%	Silt/%	Sand/%	Permeability Code	Structure Code	(Fine sand+silt/%)×(100−Clay/%)	Organic matter/%	Y Factor
F1	8.01	63.38	28.61	3	3	8462.16	0.88	0.53
F2	9.4	53.53	37.07	3	3	8208.36	1.56	0.67
F3	4.83	39.01	56.16	2	2	9057.33	0.73	0.74
F4	3.9	51.3	44.08	3	3	9235.21	0.19	0.86
F5	2.01	25.38	72.61	1	1	9602.04	0.47	0.76
F6	5.41	71.94	22.65	3	3	8947.27	0.90	0.78
F7	3.8	33.07	63.13	2	2	9254.44	3.27	0.58

guide table allocates coefficients based on specific land utilization criteria and the extent of vegetation coverage, the authors simplified it into the attached table (Table 4) showing the degree of soil protection according to its occupation in the basin of Assif el mal.

Regions characterized by exposed surfaces such as barren or rocky terrains receive higher coefficients, indicative of

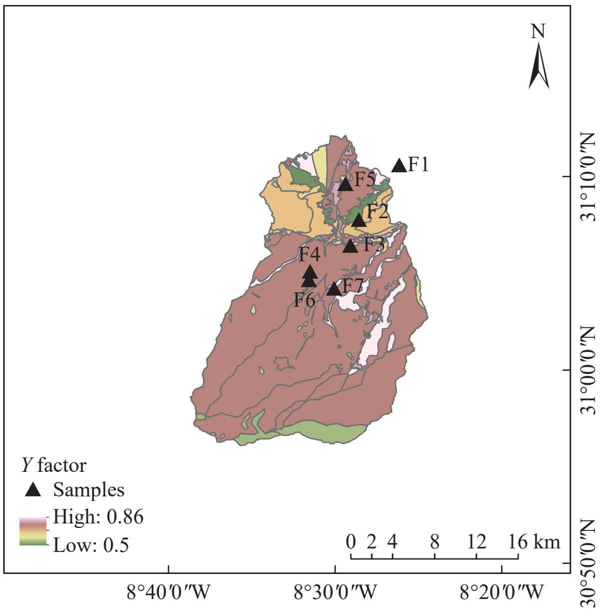

Fig. 5. Map of soil sensitivity in the Assif el mal basin.

Table 2. Temperature coefficient for each station.

Stations	Latitude	Longitude	Average temperature (1981–2021)/°C	*T*/°C
Amezmiz	−8.25	31.21	15.35	1.635
L. Takerkoust	−8.1256	31.3632	18.62	1.962
Adassil	−8.5022	31.1031	15.69	1.669
Chichaoua	−8.7635	31.548	18.95	1.995
Aghbar	−8.267	30.9327	15.35	1.635

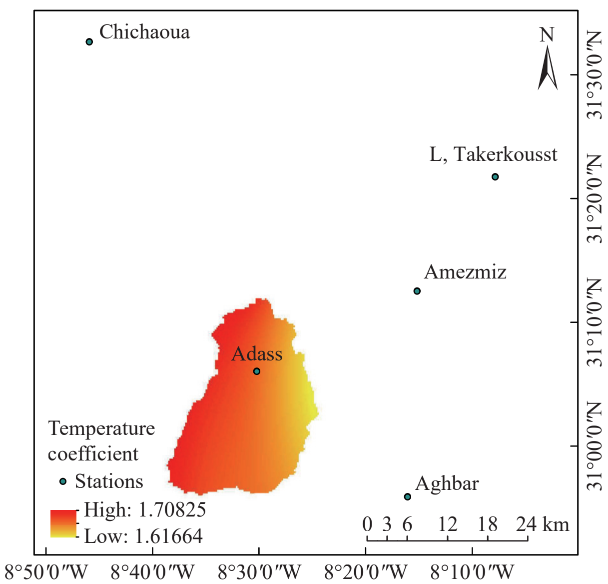

Fig. 6. Map of temperature coefficient.

their heightened susceptibility to soil erosion. Conversely, areas occupied by flourishing vegetation or human settlements tend to receive lower coefficients, reflecting a greater level of resilience against erosion. This method provides a quantifiable approach to assess erosion potential, facilitating the identification of areas at risk and enabling the strategic deployment of targeted conservation strategies.

The Assif el mal basin is characterized by a quasi-non-existence of vegetation according to the vegetation index map. The soil protection coefficient varies in parallel with it (Fig. 8).

The bare areas that constitute a large part of the basin tend to have less protection of the soil; in this case, the protection

Table 3. Mean annual precipitations.

Station	Average annual rainfall/mm
Chichaoua	191
Tahanaout	366
L. Takerkoust	245
Sidi B. Othmane	341
Ouirgane	370
Tnirt	209.4
Addouz	329
Tizi n Ghourane	485
Imm Hemmam	384
Tlat n'os	250.5
Ijoukak	327.5
Aghbar	576.5

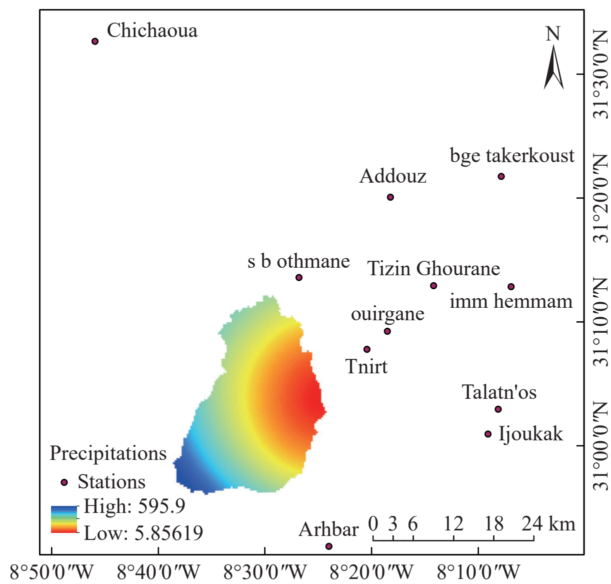

Fig. 7. Map of mean annual precipitations.

Table 4. Soil protection values according to its occupation.

Land use	Soil protection factor X_a
Villages	0
Roads	0
Dense vegetation	0.05
Moderate vegetation	0.2
Stream	0
Bare land	0.8
Rocky land	1

coefficient shows high values. Contrary to the areas where the vegetation is present, it ensures strongly this protection, and the coefficient's values are minimal.

4.1.5. Erosive state coefficient (Φ)

The erosive coefficient Φ represents the erosive state of the basin. It varies according to the distribution of the intensity of the agents involved in erosion, namely: the vegetation cover, the nature of the lithological formations, the slope, the climate and the land use.

The acquisition of field data as well as the generalized preliminary study of the Assif el mal basin allowed to establish a classification (Table 5) showing for each zone the dominant degree of erosion. At the level of Assif el mal, the values are generally between 0.1 and 1 (Fig. 9).

4.1.6. Slopes (J_a)

The slope of the land influences erosion by its degree of inclination. This has been demonstrated by several studies (Duley FL and Hays OE, 1933; Neal JH, 1938; Zingc AW, 1940; Borst HL and Woodbum R, 1940 in Ait Fora M, 1995). Indeed, the increase of the slope accentuates the runoff which also becomes erosive and its energy exceeds that of the raindrops (Woodruff CM, 1948 in Ait Fora, 1995; Zahnoun A and Al Karkouri, 2020).

In the present study, the slopes of the Assif el mal basin were generated from 3 different digital elevation models

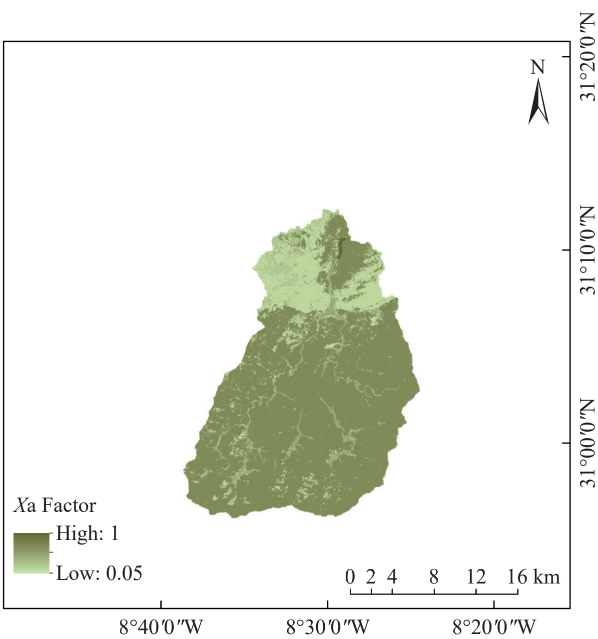

Fig. 8. Map of soil protection coefficient.

Table 5. Erosion state coefficient in the Assif el mal basin.

types and extent of erosion	erosive state coefficient
low erosion	0.1–0.2
stream erosion	0.3–0.4
erosion in rivers, ravines and alluvial deposits	0.4–0.6
surface erosion and landslide	0.7–0.8
heavy erosion throughout the basin	0.9–1

(DEM). The use of three different sources to acquire the slope data will essentially allow to test the relevance and also the efficiency of the data coming from the digital sources in the appropriate application of the models estimating the value of the erosion and the losses of the soil. With the essential purpose of comparing the results and thus determining the optimal origin of data to be used to obtain values approximately equal to the reality. The slopes map of the Assif el Mal basin was produced using three different digital elevation models (DEM) of the terrain. The purpose of this use is to be able to evaluate the effectiveness and accuracy of the data used which influence the quality of the study and provide a good representation of the field. This is critical for assessing the uncertainty of soil erosion for empirical models that use these numerical data over a wide spectrum.

The slope maps (Fig. 10) shows the distribution of the different slope classes according to their inclinations. The first map was developed using Alos palsar DEM with 12.5 m resolution. It shows a minimum value of 0% and a maximum value of 514% with an average of 50.97%. The second map was created from the Aster DEM that has a resolution of 30 m. It gives a minimum value of 0% and a maximum value of 173.5 with an average of 48.59%.The third card is generated from the Srtm DEM characterized by a resolution of 30 m, it shows a minimum value of 0% and maximum value of 330.15% with an average of 49.56%

At the level of Assif el mal, the slopes are generally strong to very strong; they occupy on average more than 50% of the whole basin (Table 6). This indicates in parallel a high susceptibility to erosion taking into account the effect of the slope.

4.1.7. Estimation of erosion in the basin of Assif el mal

In the first place, the coefficient of erosion Z of the basin of Assif el mal is calculated by applying directly the relation

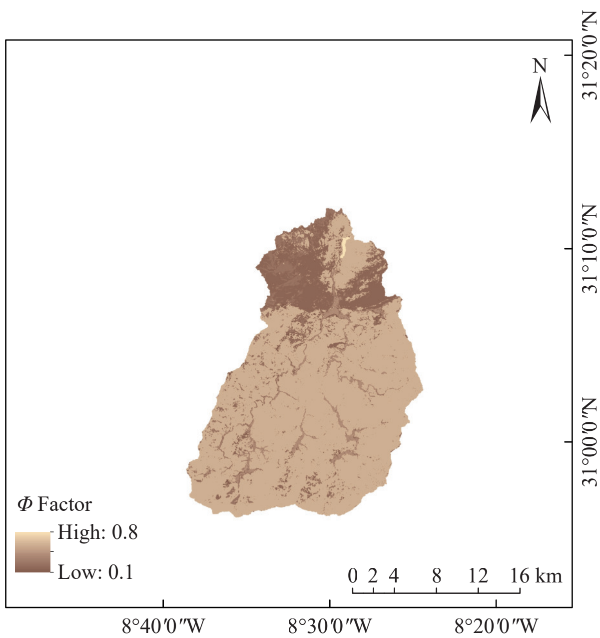

Fig. 9. Map of erosive state in the basin of Assif el mal.

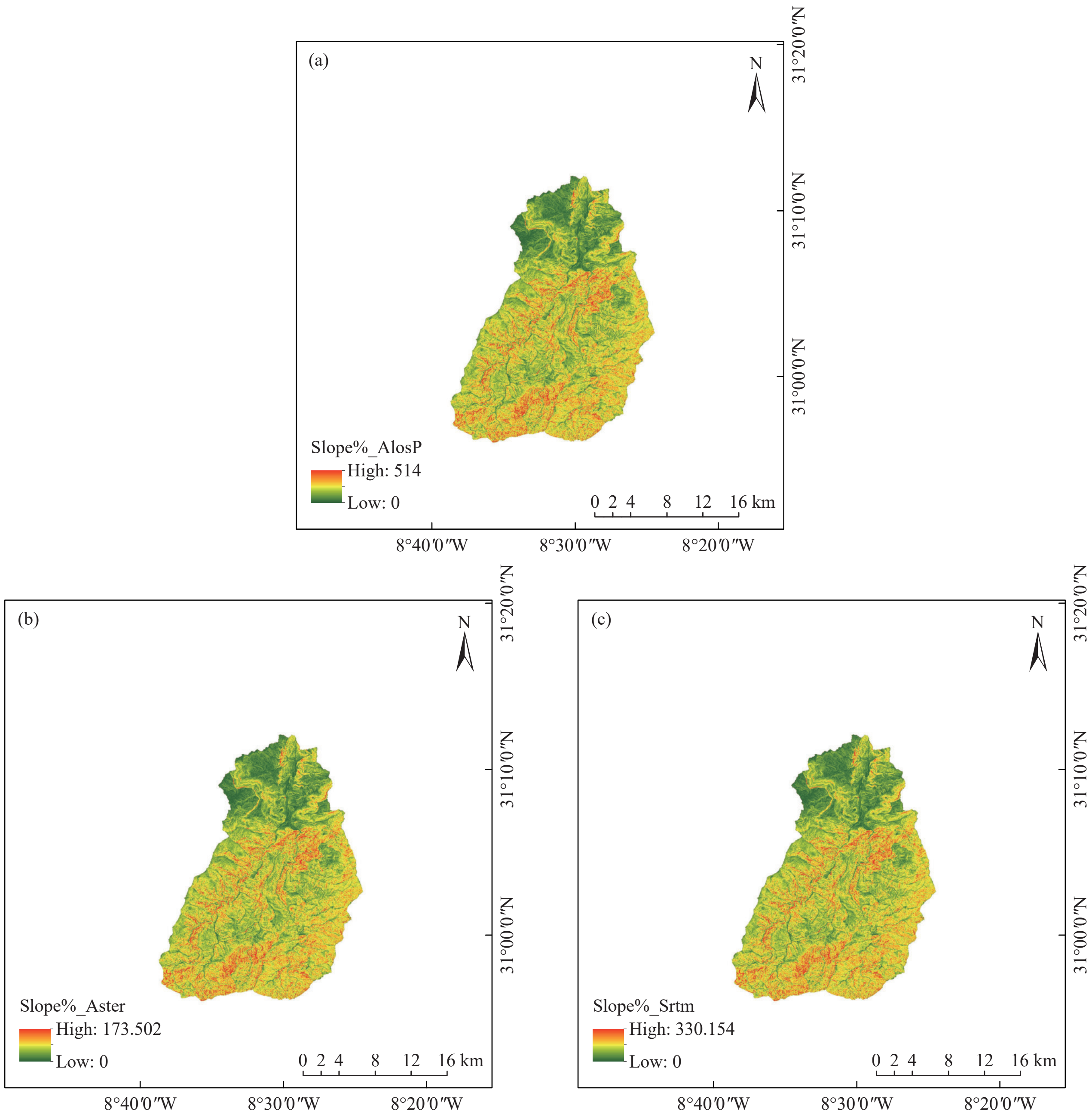

Fig. 10. Slope maps (%) of different digital elevation models (a–Alos Palsar 12.5 m; b–Aster 30 m; c–Srtm 30 m).

(1) on the software ARCGIS. In this case, the use of slopes from three different sources will give three different results (Fig. 11). The three maps yielded slightly differing results, notably highlighting the influence of the varying resolutions inherent to each DEM. These resolutions dictate the capture of finer details that play a crucial role in distinguishing and precisely identifying areas that are particularly vulnerable to erosion.

Then, applying the relation (3), will reveal the rate of soil loss in the Assif el mal basin calculated in m^3/km^2/year.

The outcomes of the study depict the spatial distribution of soil losses within the Assif el Mal basin. These distributions can generally be divided into three distinct categories, each representing varying degrees of erosion intensity. The first category encompasses areas with low erosion potential, predominantly located downstream of the basin. In these regions, the inclines of the terrain are gentle, average rainfall is modest, and the presence of vegetation cover acts as a protective barrier for the soil. The second category involves regions of moderate erosive potential, while

Table 6. Slope classes and areas.

	Slope_Alos Area		Slope_Aster Area		Slope_Srtm Area	
	km^2	%	km^2	%	km^2	%
0−5%	2.68	0.6	3.37	0.8	3.09	0.7
5%−15%	23.16	5.5	25.09	5.9	25.03	5.9
15%−45%	150.12	35.9	156.87	37.1	154.31	36.4
45%−80%	189.91	45.4	204.1	48.2	201.52	47.5
80%−100%	35.41	8.5	28.3	6.7	29.37	6.9
>100%	17.11	4.1	5.47	1.3	10,95	2.6

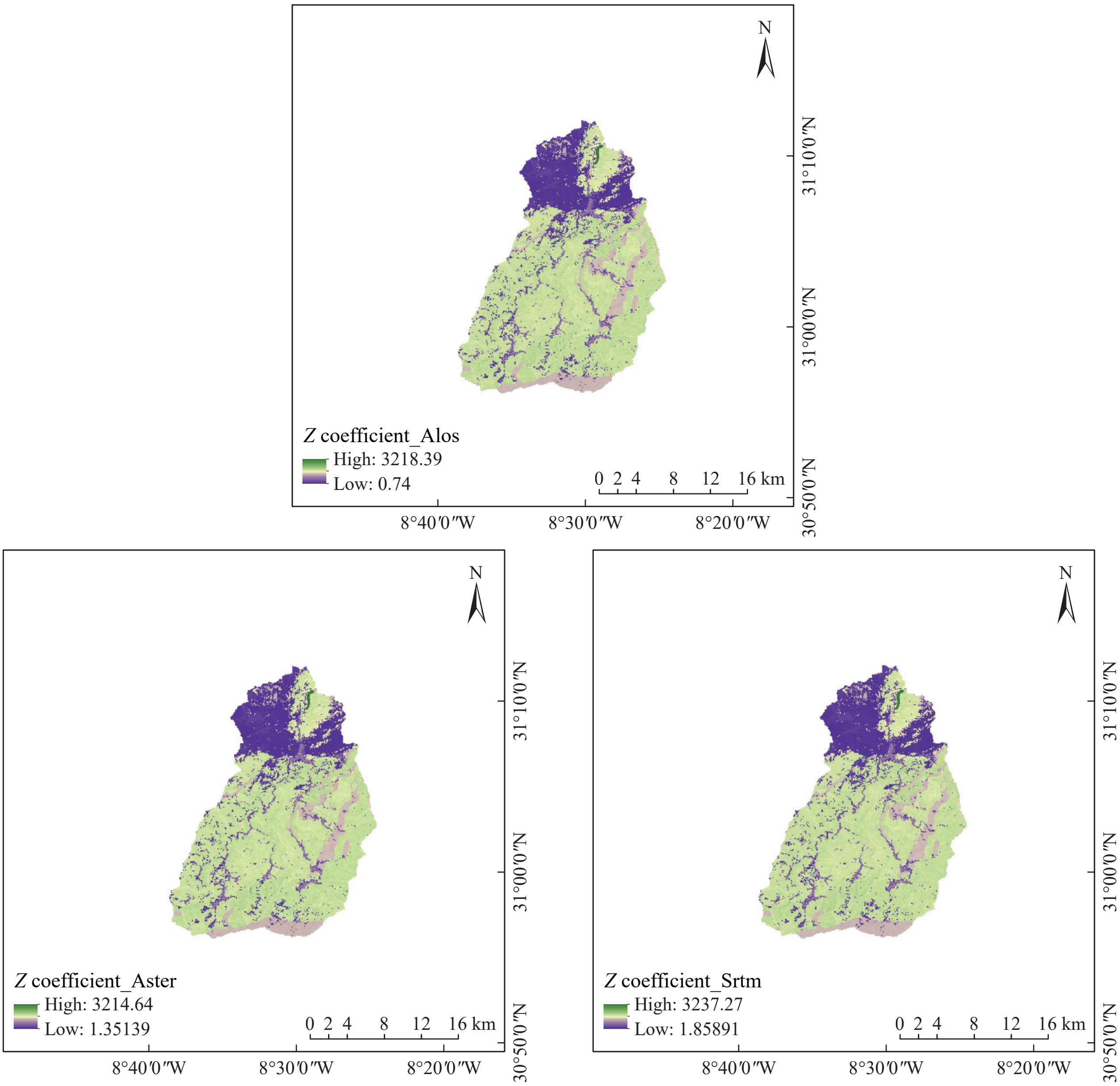

Fig. 11. Maps of the coefficient of erosion *Z*.

the third category pertains to areas with very high erosion intensity. The latter is predominantly found in the upstream portion of the basin, characterized by its challenging terrain features.

The table categorizing soil loss rates in the basin resulting from the three DEMs of varying resolutions presents the outcomes portrayed in the erosion extent maps (Fig. 12). The obtained results exhibit consistent classes (Table 7). In the realm of very low erosion classes, all DEMs yield nearly identical percentages, with a slight disparity noted for Alos Palsar. Moderate erosion risk classes, however, exhibit erosion rate estimates influenced by the DEM's resolution. Both Aster and Srtm DEMs, sharing the same resolution, display closely aligned percentages. Meanwhile, for high erosion risk classes, slight deviations emerge between Srtm and Aster DEMs, with Alos Palsar DEM displaying an intermediate value.

Eventually, the variation in erosion assessment outcomes utilizing the three DEMs was notably influenced by the heightened resolution of Alos Palsar. This enhanced resolution facilitates intricate terrain representation, aiding in precise identification of erosion-prone zones and subtle alterations. This finer resolution enables more accurate erosion pattern assessment, potentially capturing localized erosion events that might elude coarser-resolution DEMs. While Srtm's resolution is comparatively coarser than Alos Palsar, it still furnishes a reasonable overview of erosion patterns. Although it might not capture fine-scale variations as effectively, it contributes insights into broader-scale erosion trends across the region. Notably, Aster's optical sensor data, obtained at a 30 m resolution, might encounter influences from vegetation cover and lighting conditions, potentially affecting accuracy in certain zones. Consequently, erosion assessment results derived from Aster might exhibit

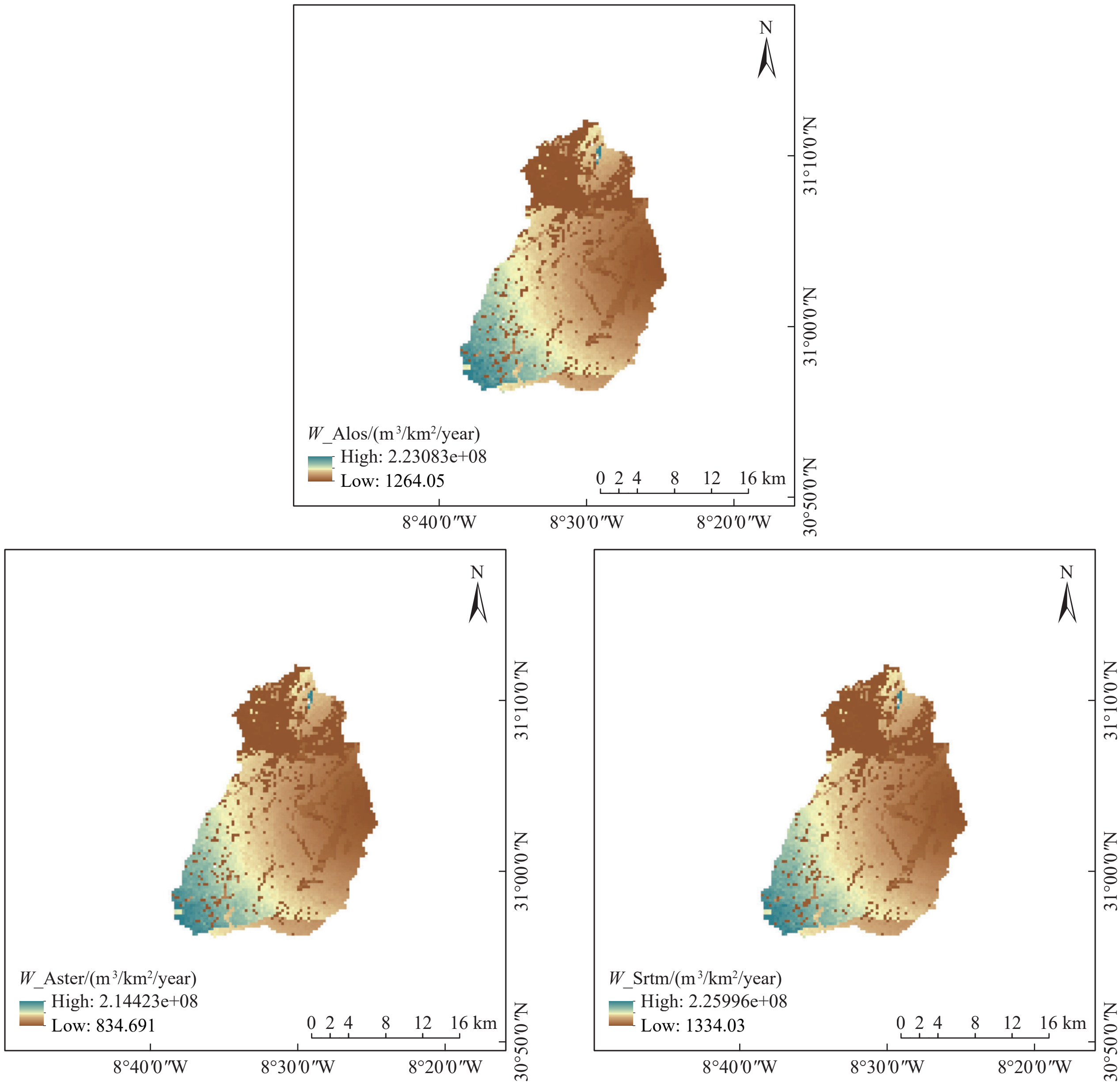

Fig. 12. Maps of soil loss in the Assif el mal basin.

Table 7. Classification of soil loss rates.

	ALOS_PALSAR		ASTER		SRTM	
	Area/m^2	%	Area /m^2	%	Area/m^2	%
1 Low	243152773	58.6	245215362	59.3	245077343.5	59.2
2 Medium	89644319.2	21.6	92276737	22.3	91113455.3	22
3 High	82797882	20.0	80885180	19.6	83427914.3	20.1

limitations in regions marked by dense vegetation or shadows, potentially leading to underestimation or overestimation of erosion.

In general, the higher resolution of Alos Palsar DEM enhances precision in erosion assessment, facilitating detailed insights and precise outcomes by effectively delineating relevant areas. In contrast, Srtm and Aster provide broader perspectives due to their coarser resolutions.

4.2. Discussions

The application of the Gavrilović's Epm model in this study has yielded valuable insights into sediment erosion and transportation rates resulting from various forms of water erosion within the Assif el Mal basin. This methodological approach has enabled a comprehensive assessment of the intricate processes involved in soil loss and sediment movement.

The study commenced by analyzing key criteria that exert pivotal control over the development of this natural phenomenon. These criteria encompass Rainfall, Slopes, Temperature, Vegetation Cover, Erosive States, and Soil Sensitivity. Calculations were conducted on each criterion, forming the foundation for susceptibility maps (Figs 5, 6, 7, 8, 9, 10). These maps vividly illustrate the extent and distribution of each factor within the basin.

Through the integration of these contributing factors via Geographic Information Systems (GIS) using Arcgis, the ultimate erosion map was synthesized. This composite representation offers a holistic depiction of spatial erosion vulnerability patterns within the watershed.

Sedimentation yield within the watershed was categorized into five distinct classes: Very Low, Low, Medium, High, and Very High. These categories correspond to the combined influence and distribution of factors governing erosion. Approximately 59% of the total area displayed low to very low potential soil losses, while 22% demonstrated moderate vulnerability. Notably, 19.9% of the land area exhibited high to very high potential for soil loss.

The adoption of the EPM model, along with other empirical models for erosion estimation, heavily relies on manipulating digital data sources such as satellite imagery, Digital Elevation Models (DEM), and geospatial datasets. This data-driven approach underpins the precision and efficacy of the model's results, providing a foundation for informed decision-making in territorial management and risk mitigation.

Notably, this study evaluated the impact of utilizing three distinct DEM sources to assess erosion risk accuracy. The focal point of this assessment was slope estimation, a pivotal morphometric parameter influencing water erosion vulnerability. Comparing slope values from these diverse sources facilitated a nuanced analysis, pinpointing the most accurate source aligning with real-world conditions. Discrepancies in slope values had a pronounced influence on soil loss estimations derived from the application of the EPM model.

Beyond Digital Elevation Models (DEMs), the accuracy of various other parameters also presents inherent challenges, affecting the precision of model evaluation results. The assessment and calculation of parameters contributing to the empirical EPM model revealed issues, such as lower-quality precipitation and air temperature maps. Recognizing these limitations underscores their potential impact on result effectiveness. Thus, emphasizing the collective accuracy of parameters including rainfall, slope, temperature, vegetation cover, erosive states, and soil sensitivity contributes to the holistic assessment of erosion dynamics. The accuracy of these constituent parameters shapes the overall reliability of the Garvrilovic Epm model’s predictions.

Undoubtedly, DEMs play a pivotal role in shaping evaluation parameters, particularly slope determination. Therefore, a preliminary analysis focusing on the spatial distribution characteristics and disparities of these parameters derived from diverse data sources is essential. Undertaking this granular examination uncovers the nuanced influence exerted by DEMs on multiple facets of the model's performance.

The resulting maps vividly illustrate the spatial distribution of water erosion-induced sedimentation rates across the Assif el Mal basin. Disparities in soil loss distribution across the three maps underscore the role of each factor’s occurrence.

Erosion and soil loss stem from complex interactions between natural and human factors. Natural elements like rainfall, wind speed, and topography influence erosion patterns. Steep slopes accelerate runoff and erosion, while wind transports soil particles. Vegetation cover stabilizes soil with roots, reducing erosion vulnerability. On the human side, activities like deforestation, urbanization, and agriculture exacerbate erosion. Vegetation removal exposes soil to erosive forces, construction alters drainage pathways, and improper farming practices leave soil susceptible.

A comprehensive analysis examines both natural and human factors contributing to the erosion landscape. The interplay between climatic conditions, geology, topography, land use, and anthropogenic activities shapes erosion susceptibility. Understanding these intricacies enriches comprehension of erosion dynamics and informs effective measures to mitigate erosion risks.

Erosion risk variance is pronounced across segments of the Assif el Mal watershed. Low values downstream contrast with elevated risk in southwest elevated terrains (exceeding 2×10^8 m^3/km^2/year). Intense rainfall, friable lithological units (Schistous formations), steep slopes, and limited vegetation cover contribute to heightened erosion intensity in its various manifestations and so is vulnerability.

Quantifying erosion rates, exemplified by Alos palsar 12.5 m, yields values spanning from 1264 to 223082992 m^3/km^2/year, averaging 53357533 m^3/km^2/year. Similarly, Aster 30 m records erosion rates ranging between 864 and 214422896 m^3/km^2/year, with an average of 53065195 m^3/km^2/year. Likewise, Srtm 30 m quantifies soil losses ranging from 1334 to225996032 m^3/km^2/year, averaging 53394594 m^3/km^2/year.

These findings underscore the profound impact of erosion's varying intensity within the study area. Disparities elucidated in this study emphasize the pivotal role of data accuracy in precise erosion estimates. These results transcend the academic realm, substantiating the role of reliable data in effective territorial management and targeted interventions to mitigate erosion’s multifaceted impacts, particularly within vulnerable regions.

Accentuating the consequences of evaluation result discrepancies on erosion assessment across regions is imperative. Variations in parameters from different data sources lead to divergent outcomes, influencing intervention strategies and mitigation measures. Elucidating these consequences comprehensively contributes to nuanced understanding of broader implications from data accuracy variations.

This comprehensive approach, assessing parameter accuracy, DEM influence, result disparities, and exploring natural and human factors, fortifies study findings. By illuminating multifaceted dimensions underlying erosion dynamics, the study informs targeted interventions, bolsters decision-making, and cultivates a proactive approach towards erosion risk management.

5. Conclusions

The exploration of water erosion and sedimentation phenomena reveals their potential exacerbation under the influence of specific climatic and human-induced factors. Assessing such risks proves crucial, necessitating studies that account for both spatial and temporal variations to mitigate potential adverse impacts. Leveraging Geographic Information Systems (GIS) has facilitated the large-scale spatial representation of erosion, enabling in-depth analyses that differentiate zones based on their erosion levels.

The culmination of this research manifests in the study of the natural processes within the Assif el Mal basin, wherein cartographic endeavors intricately merge influential factors to depict erosion's dynamics. Although accompanied by certain limitations, mapping methodologies retain their significance as powerful tools for decision-makers and planners. By simulating regional development scenarios and devising strategies for erosion control interventions, these methods highlight areas warranting heightened attention.

Within the context of the Assif el Mal region, the application of Gavrilovic's empirical EPM model unveils the extent of erosion across each segment of the catchment basin. The findings underscore an irregular distribution of soil loss rates attributable to water erosion. Low-lying sections exhibit minimal rates (<1000 m^3/km^2/year), contrasting starkly with the upstream portions, particularly the southwestern sector boasting exceedingly high rates of loss (>200000000 m^3/km^2/year). This divergence in soil loss distribution stems from the varied impacts of individual erosion factors.

Moreover, the study's comparative assessment of digital elevation models (DEMs), pivotal numerical sources heavily utilized within the basin study, serves to evaluate their precision. This evaluation concurrently underscores their relevance and effectiveness when applied to empirical models. This exploration enhances our understanding of their utility in capturing erosion dynamics and offers valuable insights for future applications.

CRediT authorship contribution statement

Kabili Salma conceived of the presented idea. Kabili Salma, Algouti Ahmed, Algouti Abdellah and Ezzahzi Salma carried out the experiment. All authors discussed the results and contributed to the final manuscript.

Declaration of competing interest

The authors declare no conflict of interest

Acknowledgments

I extend my heartfelt gratitude to the team of the 2GRNT "Geosciences, Geotourism, Natural Hazards, and Remote sensing" laboratory within the Department of Geology at the Faculty of Sciences, Cadi Ayyad University. Their unwavering guidance and support have been instrumental throughout the research, significantly enriching the development of this work. Furthermore, I express my profound appreciation for their invaluable contributions to this endeavor. Additionally, the authors would like to express their sincere gratitude to the editorial board and reviewers for their insightful remarks and constructive suggestions.

References

Ait Fora M. 1995. Spatial modeling of water erosion in a watershed of the Moroccan Rif: Validation of the geomatics approach by sedimentology, radioactive tracers and magnetic susceptibility of sediments. Quebec, University of Sherbrooke, PhD thesis, 200.

Amini S, Rafiei B, Khodabakhsh S, and Heydari M. 2010. Estimation of erosion and sediment yield of Ekbatan Dam drainage basin with EPM, using GIS. Iranian Journal of Earth Sciences, 2, 87–173.

Black PE. 1984. Watershed Hydrology, New York, Prentice-Hall.

Borst HL, Woodburn R. 1940. Rain simulator studies of the effect of slope on erosion and runoff. Soil conservation service, SCS-TP–36, 1–36.

Da ros D, Borga M. 1997. Use of digital elevation model data for the derivation of the geomorphological instantaneous unit hydrograph. Hydrological Processes, 11, 13–33. doi: 10.1002/(SICI)1099-1085(199701)11:1<13::AID-HYP400>3.0.CO;2-M.

Duley FL, Hays OE. 1933. The effect of the degree of slope on runoff and soil erosion. Journal of Agricultural Research, 45, 349–360.

Efthimiou N, Lykoudi E. 2016. Soil erosion estimation using the Epm model. Bulletin of the Geological Society of Greece, 50, 305–314. doi: 10.12681/bgsg.11731.

El Badaoui K, Algouti A, Algouti Ab, Adaze E. 2021. Erosion Potential Method (Gavrilović Method): Methodological improvements and application in Toudgha River catchment, southeast of Morocco. International Journal Water Sciences and Environment Technologies, 6(1), 114–123.

EL Bouhali A, Amyay M, El Ouazani Echa-chahdi K. 2017. The mapping of the risk of water erosion in the watershed of the Boumlal wadi (central rif-morocco) using the "Epm" model. Geomaghreb, 13, 15–24.

Elirehema Y. 2001. Soil water erosion modeling in selected watersheds in Southern Spain. Enschede, IFA, ITC.

El Mouatassime S, Boukdir A, Karaoui I, Goran Š. 2019. Modelling of soil erosion processes and runoff for sustainable watershed management: case study Oued el Abid watershed, Morocco. Agriculture & Forestry, 65(4), 241–250. doi: 10.17707/AgricultForest.65.4.22.

Gavrilovic S. 1957. Classification of Torrents in Grdelica Canyon and Quantitative Regime of TorrentBorne Sediments, Beograd.

Gavrilovic S. 1966. Methodology for Classification of Erosion Processes and Mapping of Eroded Areas. Stage I, Beograd, Institute Jaroslav Černi.

Gavrilovic S. 1972. Engineering of Torrents and Erosion. Journal of Construction (Special Issue). Belgrade, 1–292. (In Serbian)

Gavrilovic Z, Stwfanovic M, Milovanovic I, Cotric J, Milojevic M. 2008. Torrent classification- base of rational management of erosive regions, XXIVth Conference of the Danubian Countries, Bled, Slovenia

Kabili S, Algouti A, Algouti Ab, Agli S, Ikiss K. 2023. Contribution of GIS and Remote Sensing for the Mapping, Analysis and Forecasting of susceptible areas to erosion in the Assif El Mal Watershed. Indian Journal of environmental protection IJEP, 43(1), 41–47.

Kabili S, Algouti A, Algouti Ab, El Ghouat A. 2023. Quantification of water erosion using empirical models RUSLE and EPM in the Rheraya basin in the High Atlas of Marrakech. Distater advances, 16(5), 19–28. doi: 10.25303/1605da019028.

Khal M, Algouti Ab, Algouti A, Akdim N, Sergey A, Stankevich, Massimo Menenti. 2020. Evaluation of open Digital Elevation Models: estimation of topographic indices relevant to erosion risk in the Wadi M’Goun watershed, Morocco. AIMS Geosciences, 6(2), 231–257. doi: 10.3934/geosci.2020014.

Kishan SR, Anil KM, Vinay KS. 2012. Comparative evaluation of horizontal accuracy of elevations of selected ground control points from ASTER and SRTM DEM with respect to CARTOSAT-1 DEM: a case study of Shahjahanpur district, Uttar Pradesh, India. Geocarto Int 28, 439–452. doi: 10.1080/10106049.2012.724453

Liu GD, Wei MH, Yang Z, Xiao HY, Zhang YH, Fang NN. 2023. Relationship between spatio-temporal evolution of soil pH and geological environment/surface cover in the eastern Nenjiang River Basin of Northeast China during the past 30 years. China Geology, 6(3), 369–382. doi: 10.31035/cg2022062.

Neal JH. 1938. The effect of the degree of slope and rainfall characteristics on runoff and soil erosion. Soil science society of America journal, 2(C), 525–532. doi: 10.2136/sssaj1938.036159950002000C0083x.

Sadiki A, Bouhlassa S, Auajjar J, Faleh A, Macaire JJ. 2009. Use of a GIS for the evaluation and mapping of erosion risks by the Universal Soil Loss Equation in the Eastern Rif (Morocco): case of the Boussouab wadi watershed. Bulletin of the Scientific Institute, Rabat, Earth Sciences section, n°26, 69–79.

Toy TJ, Foster GR, Renard KG. 2002. Soil Erosion; Processes, Prediction, Measurement, and Control. John Wiley & Sons, Inc., New York.

Woodruff CM. 1948. Erosion in relation to rainfall, trop caver, and slope on a greenhouse plot. Soil science society of America journal, 12(C), 475–478. doi: 10.2136/sssaj1948.036159950012000C0106x.

Zahnoun A, Al karkouri J. 2020. Estimation & Cartography the Water Erosion by Integration of the Gavrilovic “Epm” Model using a Gis in the Mediterranean Watershed: Oued Tleta (Western Rif, Morocco). European Journal of Scientific Research, 155(3), 265–278.

Zingc AW. 1940. Degree and length of land slope as it affects soil loss and runoff. Agricultural Engineer, 21(2), 59–64.